

CHARACTERIZATION OF DIESEL MODEL FUEL SPRAYS IMPINGING ON A TEMPERATURE CONTROLLED WALL USING RAPID THERMOCOUPLES AND PDPA (PHASE DOPPLER PARTICLE ANALYZER)

A. Magnusson, T Joelsson, F. Turcan and S. Andersson

Department of Applied Mechanics, Chalmers University of Technology, Göteborg, Sweden

E-mail: alfhugo@chalmers.se, Phone: +46(0)31-7721419

ABSTRACT

In DI diesel engines the spray-wall interaction has been found to influence the rate of heat release and the formation of emissions. Experimental and numerical studies of sprays impinging on a wall have shown that the heat transfer and droplet size and velocity distributions vary when there is a change of such parameters as wall temperature, air temperature, injection pressure and distance to the wall. The objective of this work is to experimentally study how the surface temperature of a wall and different air temperatures affect the properties of an impinging spray of a two-component model fuel (IDEA) that consists of 70 % *n*-decane and 30 % α -methylnaphthalene. The experiments were performed in the high-pressure, high-temperature (HP/HT) spray rig at Chalmers. Air temperatures were chosen to achieve both evaporating and non-evaporating conditions of the fuel. The air pressure was adjusted to give the same density for all cases. A standard common rail system controlled by a solenoid valve together with a single-hole nozzle was used for two different fuel injection pressures.

INTRODUCTION

A major issue in the designing process of internal combustion engines is achieving good combustion efficiency and low pollutant emissions. For direct injected engines this target is strongly related to the injection process, spray formation and spray-wall interaction. In particular, a spray direct injected into the cylinder can reach the walls of the combustion chamber both in small bore engines, where the distance between the injector hole and the walls is small, and in large unit displacement engines, in which a considerable amount of fuel is usually injected each stroke.

This phenomenon, wall wetting or spray impingement might lead to incomplete evaporation and burning of wall films which may enhance soot formation and increase unburnt hydrocarbons. This effect becomes more relevant under full load or cold start, see [1] and [2]. Spray-wall interaction during cold start was also studied experimentally by Osaka et. al., [3], in investigations of how different injection strategies influenced NO_x and white smoke emissions. Lippert et al., [4], made a numerical study of the same subject, looking into the importance of parameters such as location and angle of impingement. That spray-wall interaction is an important parameter, both during and before the start of combustion in an engine, was stated by Matsson et al., [5] and [6], whom showed that the heat release can be influenced when the fuel jet reaches the wall.

Injection early in the compression stroke of an engine gives a spray that penetrates far and evaporates moderately. In order to avoid the negative effects of spray impingement, different injection strategies can be employed. Zhang et al. [7] examined the fuel distribution and mixing process when the liquid and vapour penetration impinged on a flat wall mounted in a spray rig. They used a split injection strategy and found that the fuel mass injected in each pulse and the dwell time between them were important parameters.

Several groups have used PDA/PDPA to characterize droplet size and velocities [8], [9], [10], and sometimes in combination with heat transfer measurements. Meingast et al. [10] used a single component fuel in a high-pressure/high-temperature spray rig. They discovered, inter alia, that higher wall temperature gives stronger wall-jet vortices and higher droplet velocities and great changes in the droplet size distributions. Another result was that higher wall temperature gives smaller mean diameters of the diesel droplets.

Studies of impinging sprays, under conditions that can be found in a reciprocation DI diesel engine, have been performed for different fuels and with different experimental and numerical methods by Magnusson and Montorsi et al., see [11], [12], [13], [14] and [15].

Results from these investigations have demonstrated that the different fuels used in the experiments have characteristics that behaves in a similar way for a relatively wide range of air temperatures and air pressures, before and after wall-impingement; and also that numerical simulations of different diesel fuel sprays are capable to predict some properties with good agreement while other needs to be improved.

To improve future CFD-modelling of impinging diesel fuel sprays and increase the knowledge of spray-wall interaction related phenomena, an investigation of diesel fuel spray characteristics have been performed. The present paper focuses on the spray-wall impingement process under conditions that can be found in DI diesel engines, in this case with temperature conditions close to the upper boiling point of the fuel.

The objective of the work is to characterize and compare the spray-wall interaction and heat transfer of a two-component model fuel (IDEA) for different wall temperatures using one optical method (Phase Doppler Particle Analyzer) together with surface mounted, rapid thermocouples.

EXPERIMENTAL SETUP

The experimental study was carried out in the High-Pressure/High-Temperature (HP/HT) spray rig at Chalmers, Fig. 1. It consists of a spray chamber with optical access, a fuel system, data acquisition and control systems together with an optical system suitable for spray diagnostics and a temperature-controlled wall with rapid thermocouples for temperature measurements on the wall surface.

Spray chamber

The spray chamber consists of two cylindrical shells: an outer shell of thick steel to withstand pressure and a thin inner liner to give a measurement volume of approximately 1 dm^3 , Fig. 2. Depending on the optical method chosen, three or four windows with a visibility area of approximately $40 \times 100 \text{ mm}^2$ each were used for optical access. During the experiments, one of the quartz glass windows was replaced with a "window" made of steel to enable a passage for electrical connections and the temperature controllable wall.

Wall and thermocouples

Inside the spray chamber a movable, temperature-controlled wall was placed. The distance between the wall and the nozzle was fix, but perpendicular to the spray axis the wall was moved in and out, in steps of 2.5 mm. In the wall there was eight coaxial thermocouples symmetrically placed to record the surface temperature from the heat transfer of the impinging sprays.

These thermocouples (type E) had a vacuum-deposited junction that offered a response time of approximately $3 \mu\text{s}$. In the center, 5 mm below the surface, is a thermocouple placed (type K), which has a rather long response time to measure the bulk temperature of the wall.

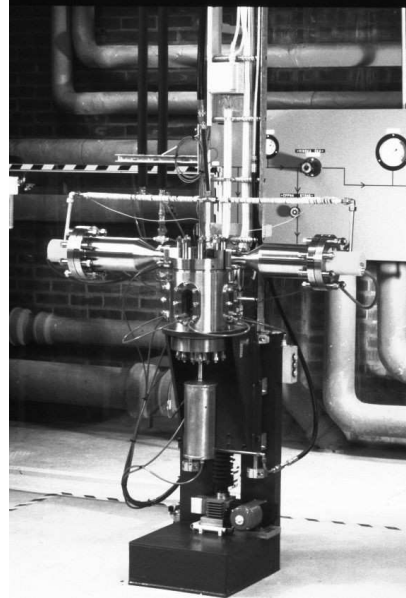


Figure 1: Chalmers' high pressure/high temperature spray rig

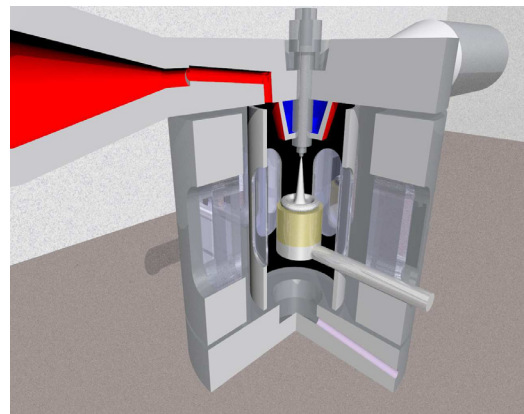


Figure 2: Drawing of the inside of the spray chamber

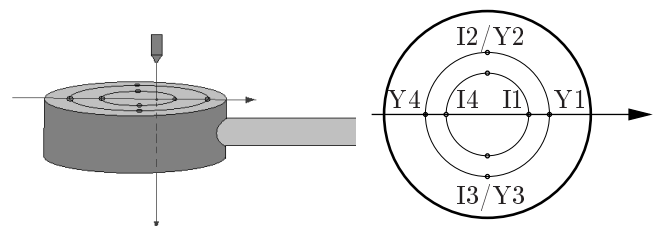


Figure 3: Drawing the movable wall with the thermocouple location

Measurement conditions

The experimental conditions were achieved by controlling air temperature, pressure and the mass flow. To deliver the heat into the spray chamber two external pre-heaters has been connected to the air intake. A third heater is placed close to the injector, to avoid cold downdraught. These three heaters could together increase the air temperature up to 900 K. The air flow was delivered by a Hamworthy 4-cylinder compressor which could created a pressure up to 100 bar.

The mass flow is low enough not to have any influence on the spray characteristics. The air pressure and air temperature in the spray chamber were for the experiments in the range of 25 to 30 bar and 300–350 °C with a density of approximately density 16 kg/m³ and in the range of 100-300 °C for the bulk temperature of the wall. The temperature of the wall was controlled by either using electrical heaters or by using compressed air for cooling.

Phase doppler particle analyzer (PDPA)

The optical measuring system used in this work was a 2-D TSI/Aerometrics PDPA-system with a TSI FSA-4000 processor. The laser used was a Coherent Innova 90 Argon-ion laser, with its two spectral lines set to 488 nm and 541.5 nm. The laser-light where separated into two lines with a acousto-optic modulator, which also divided them into four beams (with two of them frequency-shifted). The beams where focused via a transmitter into the spray chamber resulting in a measuring volume of approximately 150 μm (164 \times 155) μm .

A receiver, placed outside the spray chamber, registers the changes in intensity of the reflected and refracted light and by the PDPA-computer software (FlowSizer), the diameter and the velocity in two directions can be calculated. This software also controls the 3-dimensional traverse system where the transmitter and the receiver is placed.

Fuel system

A Bosch common-rail, single hole injector with an orifice diameter of 0.143 mm was mounted at the top of the spray chamber, see Fig. 2. The injection timing and the fuel pressure for the injections were controlled electronically and held constant throughout the experiments. To synchronize the injector with the measuring system a Stanford Research DG535 pulse generator was connected. To prevent damage on the injector and the fuel pump the fuel temperature was kept constant at approximately 25 °C by cooling the injector with cold water.

The 2-component model fuel, IDEA, a mixture of 70 % *n*-decane and 30 % α -metylnaphalene, was chosen because of its similarities with standard diesel and it contains far less components which is a necessity when making e.g. numerical simulations of the sprays. The physical behavior of IDEA and its component are listed in Table 1.

Table 1: Fuel properties at 20 °C if nothing else stated

Main physical data		Fuel	Components	
Property	Unit	IDEA model fuel	<i>n</i> -decane C ₁₀ H ₂₂	α -methyl-naphthalene C ₁₁ H ₁₀
Density	kg/m ³	798.4 @ 25 °C	730.3	1020.8
Kinematic viscosity	mm ² /s	1.72 @ 25 °C	1.28	3.27
Surface tension	N/m	24.2 · 10 ³ @ 25 °C	23.8 · 10 ³	40.0 · 10 ³
Boiling point	°C	–	174	244
Refractive index	–	1.48	1.4113	1.6174

Refractive index

When measuring with the optical system, PDPA, the software require a refractive index defined for the fuel used. Since no data was found for the blend of the two components of the fuel, a set of measurement was conducted with a multiskop (Optrel), see [16]. There the refractive index was calculated by using the multiskops function ellipsometry [17]. The two liquids were tested with this method at five different concentrations.

Two concentrations of the mixture have a known refractive index thus they were 100 % *n*-decane, refractive index, $n = 1.4113$ and 100 % α -methyl-naphthalene, $n = 1.6174$. The other three fluid mixtures have different concentrations which gave an almost linear relation of the refractive index and for the chosen concentration a refractive index of 1.48 was set, see Table 1.

ANALYSIS

Data validity – Surface temperature measurements

Due to unnatural oscillations, noise and false or pseudo signals, some of the samples have to be sorted out from the ensemble of collected data before further processing, since an incorrect value will influence the others too much in the averaging process. This separation is done by in-house Matlab algorithms that use built-in standard statistical functions, see [18].

Also, a shifting of the signals in the x and y direction (time and temperature) must be performed. The reason for this is that the surface temperature of the wall is constant and uniform but after the signals are amplified, the level of each channel cannot be set to zero before acquiring the data. The time when the temperature starts to change must be shifted to take care of the variations of each spray regarding start of injection and also the differences in the total penetration time until the spray impinges the wall. Figure 4 shows an example of an ensemble of different measured temperatures with different kinds of disturbances.

After sorting out samples that are not statistically valid, 90 samples of the total 120 are chosen for the averaging process which includes calculation of the standard deviation and arithmetic calculation of the mean value for each signal after filtering. An example of 10 samples and an average temperature curve is shown in Fig. 5.

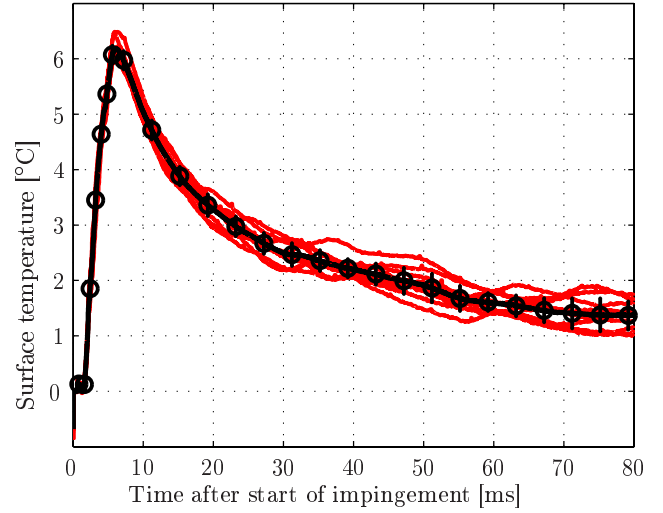


Figure 5: Temperature history of 10 samples together with averaged value and standard deviation.

Data validity – Droplet velocity and size measurements

When sampling data with the Phase Doppler Particle Analyzer one has to consider if the range of visibility of droplets is good enough. As in this case, in the front vortex outside the spray core, where the spray could be too dense or too diluted which could influence the measurements statistically. After the measurements, the data that are generated from the PDDA system can be presented as scatter plots of the diameter or the axial and radial velocity distribution, see Fig. 6.

To extract information for the axial and radial velocities were the arithmetic mean value, mode value and time for burst, calculated, see definition 1 and 2. From the measured droplets diameter were, arithmetic mean value, D_{10} , and Sauter mean diameter, SMD or D_{32} , calculated. The mean values were calculated out of a time interval of 0.20 ms from time for burst, TFB which is found when the number of droplets in the chosen time interval is higher than $\rho = 250$ samples/ms.

Definition 1 (Mode value) *The sample Mode value is the most frequently occurring data value in a defined quantity.*

Definition 2 (Time for Burst) *Time for burst is the time after injection when the first burst of droplets arrive to a defined measuring volume.*

From the sampled data was a probability density function, PDF, calculated. Calculation of these PDF plots includes limits for realistically velocities and diameters. Out of the PDF plots is the mode value spotted, in addition to the mean value which could be calculated. An example of generated PDF plots are shown in Fig. 7.

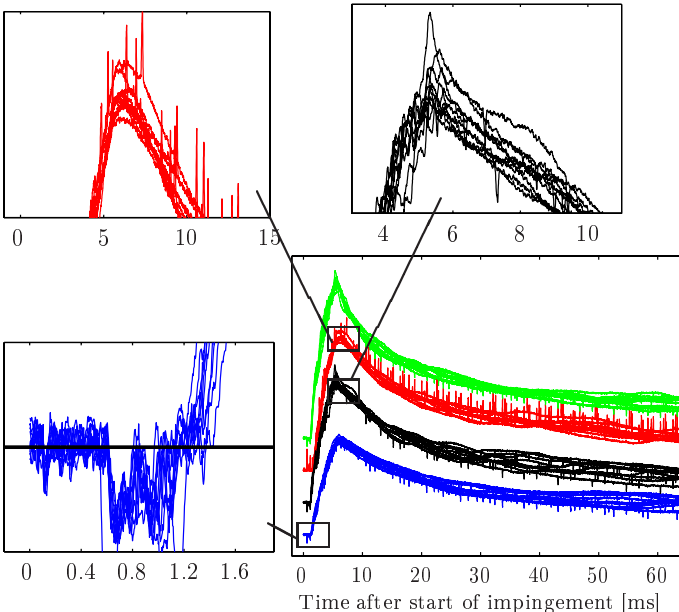


Figure 4: Ensemble of sampled temperatures from four thermocouples with different kind of disturbances.

To get more statistically trustworthy calculated velocities (axial and radially) a coincidence interval were chosen in the FlowSizer software in order to couple data from each channel together. This software feature reduces the amount of samples but increases the probability that the radial and the axial velocity are from the same droplet. This makes it possible to calculate a 2-dimensional distribution of the droplet's velocities or the distribution of the droplet's speed.

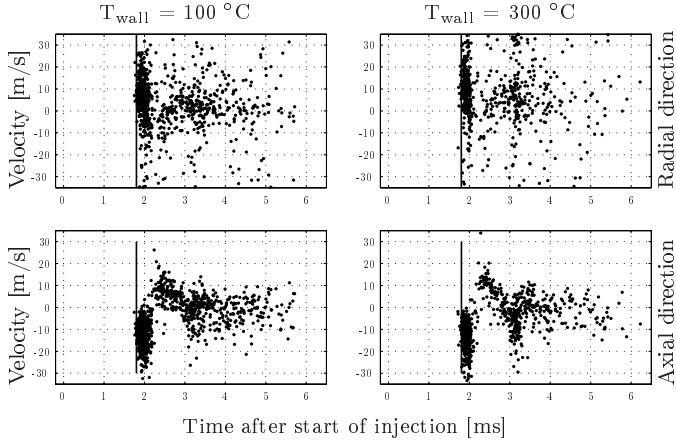


Figure 6: Scatter plot of droplet's radial and axial velocity. Air temperature = $300\text{ }^{\circ}\text{C}$ and air pressure = 26 bar.

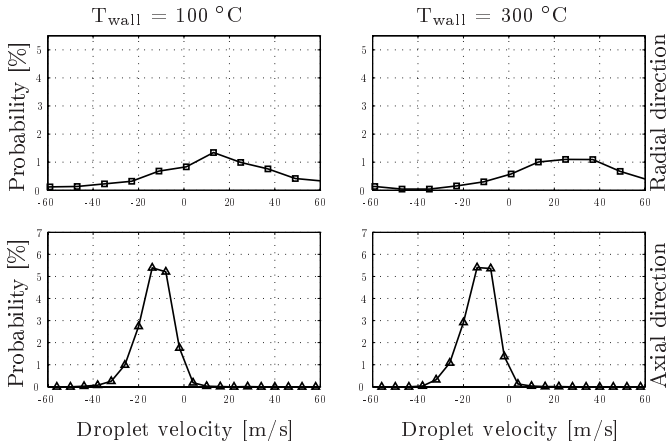


Figure 7: Velocity PDF at TFB. Air temperature = $300\text{ }^{\circ}\text{C}$ and air pressure = 26 bar.

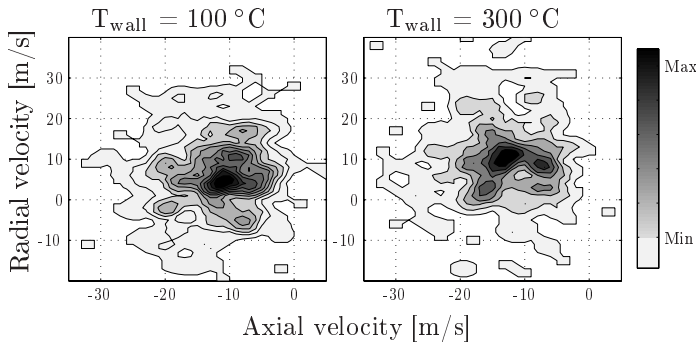


Figure 8: Droplet velocity distribution calculated from data with a coincidence interval of $10\text{ }\mu\text{s}$ in an interval of 0.2 ms after the first burst of droplets. Air temperature = $300\text{ }^{\circ}\text{C}$ and air pressure = 26 bar.

RESULTS

Surface temperature consistency

Since the wall surface temperature evolution, after impingement, has been measured at different wall positions in the HT/HP spray chamber, in such a way that the thermocouples radius (5 and 10 mm) are multiples of the wall displacement step (1.25 mm), the heat transfer from the sprays are acquired several times (provided the environmental conditions are the same), but from different thermocouples point of view.

This means that by choosing the right wall positions, it is possible to compare the four different signals together to check if the thermocouples are giving the same information at the same spatial position. This is exemplified in Fig. 3 and in Fig. 9 where the averaged results from the temperatures measured at the -5 mm position is shown, (note that only three out of four thermocouples was working for this case).

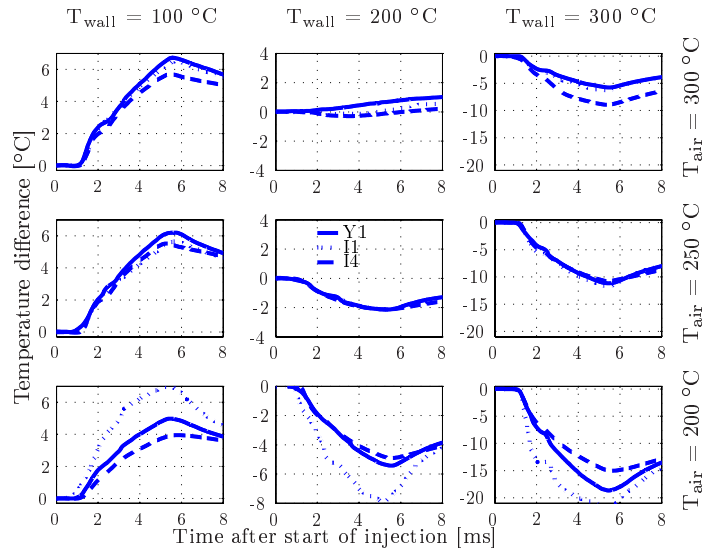


Figure 9: Averaged temperature histories measured at the same distance from the spray axis with the wall placed at three different positions. Injection pressure = 1300 bar

As can be seen in Fig. 9 the different thermocouples are not measuring the same temperature change for some of the cases, even though the experimental conditions are the same (except the wall positioning). For example, for the lowest air temperature ($T_{air} = 200\text{ }^{\circ}\text{C}$) the thermocouple at the I1 position have a much greater response than the other two even though there is an increase or decrease in temperature from the heat transfer. Another behaviour can be observed for the case when the air and the wall temperature are the highest where the thermocouple at position Y1 has a remarkable weaker decrease in temperature while the I1 and I4 thermocouple has a similar trend.

Wall alignment accuracy

The discrepancy within the accuracy of the different thermocouples is of course a dilemma when, for example, measuring the temperature with thermocouple I1, I2, I3 and I4 at the radius 5 mm from the spray axis i.e. when the wall is in the center of the spray.

Figure 10 shows the temperature development at three different wall positions close to the spray axis where it can be seen that when moving the wall along its axis, the temperature difference decreases from radius -1.5 mm to 1.5 mm for three of the thermocouples but have a relatively constant temperature difference for the fourth.

This indicates that the center of the wall is not fully aligned with the spray's axis. Comparing the number I2 and I3 temperature development does not give any answer if the wall is aligned in the spray axis since it is not clarified if either one of them gives the right value.

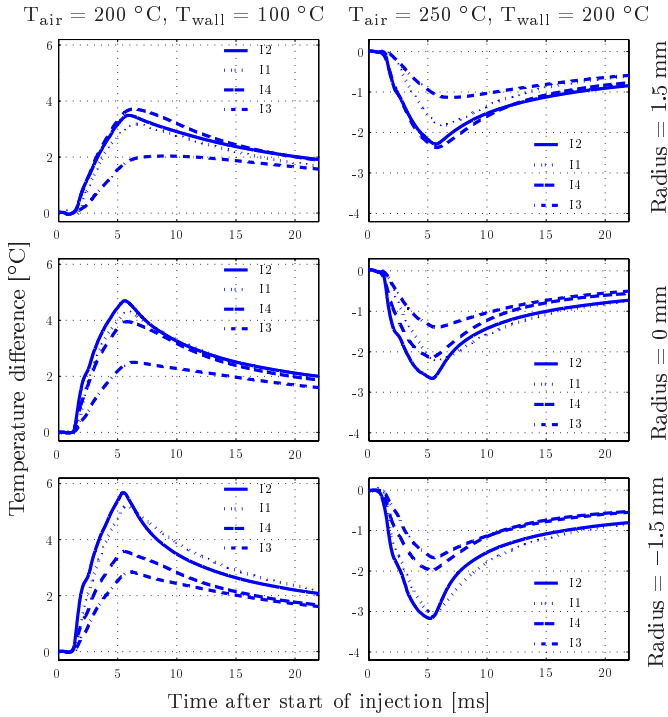


Figure 10: Averaged temperature histories measured with the inner thermocouples at three different radii from the spray axis. Injection pressure = 1300 bar

Influence of wall temperature on spray behaviour

In the study of how the wall temperature influences the spray behavior are two cases chosen to demonstrate the results calculated from the measurements.

The first case have an air temperature of 200 °C and the other 300 °C. The measurements were done at two different wall surface temperatures, 100 °C and 300 °C at two different radii $R=10$ mm and $R=18$ mm and at three different heights above the wall surface.

From the measurements are the Sauter Mean Diameter, SMD, calculated for the chosen interval, (0.20 ms after TFB). Tables 2 and 3 shows that the SMD have a tendency to increase closer to the wall surface for the case with lowest wall temperature but the opposite when the wall has the higher temperature regardless of air temperature. This indicates that the wall temperature influences the droplet size distribution to some extent. Note that at two of the measurement points the sampling rate was too low to fulfill the requirements of trustworthiness and thereby no SMD was calculated.

Table 2: Sauter Mean Diameter at $T_{\text{air}} = 200$ °C

R = 10 mm		R = 18 mm		Height [mm]
T_{wall} 100 °C	T_{wall} 300 °C	T_{wall} 100 °C	T_{wall} 300 °C	
13.6	15.0	12.2	14.6	5
14.2	14.0	13.5	14.2	3
15.3	14.1	14.0	14.1	1

Table 3: Sauter Mean Diameter at $T_{\text{air}} = 300$ °C

R = 10 mm		R = 18 mm		Height [mm]
T_{wall} 100 °C	T_{wall} 300 °C	T_{wall} 100 °C	T_{wall} 300 °C	
9.2	12.2	8.4	—	5
9.4	11.0	8.3	—	3
10.7	10.6	9.9	10.8	1

Averaged values for the axial and radial velocities from the data using the coincidence feature are presented in Table 4–7. A comparison of the average axial velocities in Table 4 and 5 shows that there are only small differences in respectively value when looking at the influence of wall temperature for each point but one can discern one trend. The closer to the wall the measurement is done the higher becomes the average velocity, except for two cases when the sample rate was too low.

Table 4: Averaged axial velocities, [m/s], at $T_{\text{air}} = 200 \text{ }^\circ\text{C}$

R = 10 mm		R = 18 mm		Height [mm]
T_{wall} 100 $^\circ\text{C}$	T_{wall} 300 $^\circ\text{C}$	T_{wall} 100 $^\circ\text{C}$	T_{wall} 300 $^\circ\text{C}$	
-5	-4	-5	-4	5
-6	-4	-7	-7	3
-7	-6	-7	-7	1

Table 5: Averaged axial velocities, [m/s], at $T_{\text{air}} = 300 \text{ }^\circ\text{C}$

R = 10 mm		R = 18 mm		Height [mm]
T_{wall} 100 $^\circ\text{C}$	T_{wall} 300 $^\circ\text{C}$	T_{wall} 100 $^\circ\text{C}$	T_{wall} 300 $^\circ\text{C}$	
-4	-5	-8	—	5
-5	-7	-10	—	3
-7	-8	-11	-11	1

Table 6: Averaged radial velocities, [m/s], at $T_{\text{air}} = 200 \text{ }^\circ\text{C}$

R = 10 mm		R = 18 mm		Height [mm]
T_{wall} 100 $^\circ\text{C}$	T_{wall} 300 $^\circ\text{C}$	T_{wall} 100 $^\circ\text{C}$	T_{wall} 300 $^\circ\text{C}$	
4	0	-1	-2	5
4	3	2	2	3
6	8	9	9	1

Table 7: Averaged radial velocities, [m/s], at $T_{\text{air}} = 300 \text{ }^\circ\text{C}$

R = 10 mm		R = 18 mm		Height [mm]
T_{wall} 100 $^\circ\text{C}$	T_{wall} 300 $^\circ\text{C}$	T_{wall} 100 $^\circ\text{C}$	T_{wall} 300 $^\circ\text{C}$	
3	3	0	—	5
5	3	3	—	3
5	6	10	2	1

Concerning the radial velocities a behaviour similar as for the axial velocity can be found, see Table 6 and 7 and since both the axial and the radial velocity are coupled to each other through the coincidence treatment in FlowSizer, the average speed for each case can be calculated. This gives an indication of how the droplets tends to slow down when they moves upwards but when looking at the case with the higher air temperature, 300 $^\circ\text{C}$ and closest to the wall $H=1 \text{ mm}$, the speed increases further out, from $R=10 \text{ mm}$ and $R=18 \text{ mm}$.

CONCLUSION

Temperature development

A new designed wall, moveable in the perpendicular direction to the spray axis, was used to measure the temperature change at the wall from the heat transfer of impinging diesel sprays. When measuring the temperature at different spatial positions in the spray it could be found that:

- The thermocouples measured different temperatures even though they were placed at the same radius from the spray axis. The reason for this behaviour is not fully understand but different reasons can be proposed. One is that the thermocouples are not mounted exactly in the wall compared to its surface. Another reason could be that, instantaneously speaking, the thermocouples do not measure the same since the measurements have not been performed at the same time, which is a matter of repeatability about the apparatus used.
- By scanning through the spray, close to its centerline, it was possible to locate the spray axis, which in this investigation showed to be slightly off axis. This incorrectness has its explanations in the design of the spray chamber since the injector might be tilted slightly when mounted.

Droplet behaviour

The experimental study of the spray behaviour from diesel sprays impinging on a temperature controllable wall showed that the wall temperature had some influence on the droplet size and velocity distribution. Comparing the effect of wall temperature for different air temperatures and spatial positions showed that:

- The Sauter mean diameter increased closer to the wall surface for the case with lowest wall temperature but the opposite when the wall has the higher temperature regardless of the chosen air temperature.

- For the averaged radial and axial velocity no influence due to the different wall temperature could be found. When measuring at different spatial positions one can notice that the averaged velocity of the droplets tends to decrease in the upward direction but increase further out from the spray axis.

ACKNOWLEDGEMENTS

The authors would like to acknowledge STEM (Swedish Energy Agency) for their financial support and laboratory personnel for their assistance.

REFERENCES

- [1] M.A. Gonzalez, G.L. Borman and R.D. Reitz, A Study of Diesel Cold Starting using Both Cycle Analysis and Multidimensional Calculations, *SAE paper 910180*, (1991).
- [2] A.K. Zahdeh, N. Henein and W. Bryzik, Diesel Cold Starting: Actual Cycle Analysis Under Border-Line Conditions, *SAE paper 900441*, (1990).
- [3] I. Osuka, M. Nishimura, Y. Tanaka and M. Miyaki, Benefits of New Fuel Injection System Technology on Cold Startability of Diesel Engines – Improvement of Cold Startability and White Smoke Reduction by Means of Multi Injection with Common Rail Fuel System (ECD-12), *SAE paper 940586*, (1994).
- [4] A.M. Lippert, D.W. Stanton, R.D. Reitz, C.J. Rutland and W.L.H. Hallett, Investigating the Effect of Spray Targeting and Impingement on Diesel Engine Cold Start, *SAE paper 2000-01-0269*, (2000).
- [5] A. Matsson, L. Jakobsson and S. Andersson, The Effect of Elliptical Nozzle Holes on Combustion and Emission Formation in a Heavy Duty Diesel Engine, *SAE paper 2000-01-1251*, (1999).
- [6] A. Matsson, L. Jakobsson and S. Andersson, The Effect of Non-Circular Nozzle Holes on Combustion and Emission Formation in a Heavy Duty Diesel Engine, *SAE paper 2002-01-2671*, (2002).
- [7] Y. Zhang, T. Ito and K. Nishida, Characterization of Mixture Formation in Split-Injection Diesel Sprays via Laser Absorption Scattering (LAS) Technique, *SAE paper 2001-01-3498*, (2001).
- [8] C. Arcoumanis, and J-C. Chang, Flow and Heat Transfer Characteristics of Impinging Transient Diesel Sprays, *SAE paper 940678*, (1994).
- [9] E. Schünemann, S. Fedrow and A. Leipertz, Droplet Size and Velocity Measurement for the Characterization of a DI-Diesel Spray Impinging of a Flat Wall, *SAE paper 982545*, (1998).
- [10] U. Meingast, M. Staudt, L. Reichelt, U. Renz and F.A. Sommerhoff, Analysis of Spray/Wall Interaction Under Diesel Engine Conditions, *SAE paper 2000-01-0272*, (2000).
- [11] A. Magnusson, S. Jedrzejowski and S. Andersson, Spray-wall interaction: an experimental study of multiple injections of standard diesel, *20th Ilass Europe '05*, (2005).
- [12] A. Magnusson, S. Jedrzejowski and S. Andersson, Spray-wall Interaction: Diesel Fuels Impinging on a Tempered Wall, *SAE paper 2006-01-1116*, (2006).
- [13] A. Magnusson, S. Jedrzejowski and S. Andersson, Comparison of Heat Transfer and Spray Characteristics for a Model Fuel and Standard Diesel Sprays Interacting with a Temperature-Controlled Wall, In *THIESEL 2006*, (2006).
- [14] L. Montorsi, A. Magnusson and S. Andersson, A Numerical and Experimental Study of Diesel Fuel Sprays Impinging on a Temperature Controlled Wall, *SAE paper 2006-01-3333*, (2007).
- [15] L. Montorsi, A. Magnusson and S. Andersson, Numerical and Experimental Analysis of the Wall Film Thickness for Diesel Fuel Sprays Impinging on a Temperature Controlled Wall, *SAE paper 2007-01-0486*, (2007).
- [16] T. Joelsson, PDPA measurements of diesel fuel droplets impinging on a temperature controlled wall, Master's Thesis, Chalmers University of Technology, (2007).
- [17] M. Harke, R. Teppner, O. Schultz and H. Motschmann, Description of a single modular optical setup for ellipsometry, surface plasmons, waveguide modes, and their corresponding imaging techniques including Brewster angle microscopy, *American Institute of Physics*, (1997).
- [18] F. Turcan, Temperature measurements of diesel sprays impinging on a temperature controlled wall, Master's Thesis, Chalmers University of Technology, (2008).